

**This Page is Inserted by IFW Indexing and Scanning
Operations and is not part of the Official Record**

BEST AVAILABLE IMAGES

Defective images within this document are accurate representations of the original documents submitted by the applicant.

Defects in the images include but are not limited to the items checked:

- BLACK BORDERS**
- IMAGE CUT OFF AT TOP, BOTTOM OR SIDES**
- FADED TEXT OR DRAWING**
- BLURRED OR ILLEGIBLE TEXT OR DRAWING**
- SKEWED/SLANTED IMAGES**
- COLOR OR BLACK AND WHITE PHOTOGRAPHS**
- GRAY SCALE DOCUMENTS**
- LINES OR MARKS ON ORIGINAL DOCUMENT**
- REFERENCE(S) OR EXHIBIT(S) SUBMITTED ARE POOR QUALITY**
- OTHER: _____**

IMAGES ARE BEST AVAILABLE COPY.

As rescanning these documents will not correct the image problems checked, please do not report these problems to the IFW Image Problem Mailbox.



UNITED STATES PATENT AND TRADEMARK OFFICE

UNITED STATES DEPARTMENT OF COMMERCE
United States Patent and Trademark Office
Address: COMMISSIONER FOR PATENTS
P.O. Box 1450
Alexandria, Virginia 22313-1450
www.uspto.gov

APPLICATION NO.	FILING DATE	FIRST NAMED INVENTOR	ATTORNEY DOCKET NO.	CONFIRMATION NO.
09/778,306	02/06/2001	Behrouz Farhang-Boroujeni	21046.P004	5649
7590	07/13/2004		EXAMINER	
Lawrence N. Ginsberg 907 Citrus Place Newport Beach, CA 92660			NGUYEN, DUNG X	
			ART UNIT	PAPER NUMBER
			2631	

DATE MAILED: 07/13/2004

Please find below and/or attached an Office communication concerning this application or proceeding.

RECEIVED

JUL 29 2004

Technology Center 2100

Office Action Summary	Application No.	Applicant(s)
	09/778,306	FARHANG-BOROUJENI ET AL.
	Examiner Dung X Nguyen	Art Unit 2631

-- The MAILING DATE of this communication appears on the cover sheet with the correspondence address --

Period for Reply

A SHORTENED STATUTORY PERIOD FOR REPLY IS SET TO EXPIRE 3 MONTH(S) FROM THE MAILING DATE OF THIS COMMUNICATION.

- Extensions of time may be available under the provisions of 37 CFR 1.136(a). In no event, however, may a reply be timely filed after SIX (6) MONTHS from the mailing date of this communication.
- If the period for reply specified above is less than thirty (30) days, a reply within the statutory minimum of thirty (30) days will be considered timely.
- If NO period for reply is specified above, the maximum statutory period will apply and will expire SIX (6) MONTHS from the mailing date of this communication.
- Failure to reply within the set or extended period for reply will, by statute, cause the application to become ABANDONED (35 U.S.C. § 133). Any reply received by the Office later than three months after the mailing date of this communication, even if timely filed, may reduce any earned patent term adjustment. See 37 CFR 1.704(b).

Status

1) Responsive to communication(s) filed on _____.
 2a) This action is **FINAL**. 2b) This action is non-final.
 3) Since this application is in condition for allowance except for formal matters, prosecution as to the merits is closed in accordance with the practice under *Ex parte Quayle*, 1935 C.D. 11, 453 O.G. 213.

Disposition of Claims

4) Claim(s) 1 - 41 is/are pending in the application.
 4a) Of the above claim(s) ____ is/are withdrawn from consideration.
 5) Claim(s) 1 - 15 and 25 - 41 is/are allowed.
 6) Claim(s) 16, 18, and 20 - 24 is/are rejected.
 7) Claim(s) 17 and 19 is/are objected to.
 8) Claim(s) ____ are subject to restriction and/or election requirement.

RECEIVED

JUL 29 2004

Technology Center 2100

Application Papers

9) The specification is objected to by the Examiner.
 10) The drawing(s) filed on 06 February 2001 is/are: a) accepted or b) objected to by the Examiner.
 Applicant may not request that any objection to the drawing(s) be held in abeyance. See 37 CFR 1.85(a).
 Replacement drawing sheet(s) including the correction is required if the drawing(s) is objected to. See 37 CFR 1.121(d).
 11) The oath or declaration is objected to by the Examiner. Note the attached Office Action or form PTO-152.

Priority under 35 U.S.C. § 119

12) Acknowledgment is made of a claim for foreign priority under 35 U.S.C. § 119(a)-(d) or (f).
 a) All b) Some * c) None of:
 1. Certified copies of the priority documents have been received.
 2. Certified copies of the priority documents have been received in Application No. _____.
 3. Copies of the certified copies of the priority documents have been received in this National Stage application from the International Bureau (PCT Rule 17.2(a)).

* See the attached detailed Office action for a list of the certified copies not received.

Attachment(s)

1) Notice of References Cited (PTO-892)
 2) Notice of Draftsperson's Patent Drawing Review (PTO-948)
 3) Information Disclosure Statement(s) (PTO-1449 or PTO/SB/08)
 Paper No(s)/Mail Date _____.
 4) Interview Summary (PTO-413)
 Paper No(s)/Mail Date _____.
 5) Notice of Informal Patent Application (PTO-152)
 6) Other: _____.

DETAILED ACTION***Drawings***

1. The drawings are objected to because:

On figure 3, blocks 102, 104, 106, 108, 114, 116, 118, and 120 must use descriptive language to identify each of such blocks.

A proposed drawing correction or corrected drawings are required in reply to the Office action to avoid abandonment of the application. The objection to the drawings will not be held in abeyance.

Claim Rejections - 35 USC § 103

2. The following is a quotation of 35 U.S.C. 103(a) which forms the basis for all obviousness rejections set forth in this Office action:

(a) A patent may not be obtained though the invention is not identically disclosed or described as set forth in section 102 of this title, if the differences between the subject matter sought to be patented and the prior art are such that the subject matter as a whole would have been obvious at the time the invention was made to a person having ordinary skill in the art to which said subject matter pertains. Patentability shall not be negatived by the manner in which the invention was made.

3. **Claims 16, 18 are rejected** under 35 U.S.C. 103(a) as being unpatentable over Jones et al. (US patent # 6,128,351), in view of Komatsu (US patent # 6,144,860).

Regarding claim 16, Jones et al. et al. discloses:

- an input data for receiving a known data signal (column 1, lines 53 – 54);
- an input data for receiving an unknown data signal (column 1, lines 51 – 52);

- a data combiner to produce the composite output signal having discrete data signals, wherein each discrete data signal comprising at least a portion of unknown data (column 1, line 61) and at least a portion of the known data signal (column 1, line 68).

While Komatsu discloses a signal power ratio input for receiving a power ratio signal indicating a ratio combining the unknown data signal and the known data signal (column 3, lines 18 – 32).

Therefore, it would have been obvious to one of ordinary skill in the art at the time of the invention was made to combine Jones et al. and Komatsu to improve the communication system.

Regarding claim 18, Jones et al. further inherently discloses that combiner is a frequency domain data combiner (column 1, lines 22 – 23. As the combiner for receiving OFDM modulated signals, it must be a frequency domain data combiner).

4. **Claims 20 – 24 are rejected** under 35 U.S.C. 103(a) as being unpatentable over Jones et al. (US patent # 6,128,351), Komatsu (US patent # 6,144,860), further in view of figure 1 admitted as a prior art by applicant.

Regarding claims 20 and 21, respectively, as followed by the limitations analyzed in claim 16, Jones et al. and Komatsu differ from the instant claimed invention that they do not show the step of comprising a serial to parallel converter having a plurality of outputs.

However, figure 1 admitted as a prior art by applicant discloses the serial to parallel converter (102) to provide a plurality of outputs.

Therefore, it would have been obvious to one of ordinary skill in the art at the time of the invention was made to combine Jones et al., Komatsu, and figure 1 admitted as a prior art by applicant to improve the communication system.

Regarding claim 22 and 23, respectively, as followed by the limitations analyzed in claim 21, figure 1 admitted as a prior art by applicant further discloses an inverse discrete Fourier transform module (104).

Regarding claim 24, as followed by the limitations analyzed in claim 23, figure 1 admitted as a prior art by applicant further discloses a cyclic prefix adder (108).

Allowable Subject Matter

5. **Claims 17 and 19 are objected** to as being dependent upon a rejected base claim, but would be allowable if rewritten in independent form including all of the limitations of the base claim and any intervening claims.

6. **Claims 1 – 15 and 25 – 41 are allowed.** The following is a statement of reasons for the indication of allowable subject matter:

Regarding to the claimed inventions, the prior art of record fails to show or render obvious of a multi-carrier communication system, comprising:

A transmission unit comprising:

- A data input for receiving an unknown data signal;
- A data input for receiving a know data signal;
- A power ratio signal input for receiving a power ratio signal indicating a ratio for combining unknown data and known data signals; and
- A data combiner coupled to the data input for combining the unknown and known data signals in accordance with the power ratio signal to produce a composite signal comprising discrete data signals, wherein each discrete data signal comprises at least a portion of the unknown data signal and at least a

portion of the known data combined in accordance with the power ratio signal. It also has an output adapted to provide the composite output signal to a multi-carrier transmitter transmitted a transmit signal on a communication channel, wherein the transmit signal includes the composite signal; and

A receiving unit comprising:

- A multi-carrier receiver for receiving the transmitted signal on the communication channel, having an output for providing a corresponding composite signal, wherein the composite signal comprises corresponding discrete data signals and is shaped by at least one signal shaping characteristic of the communication channel;
- A channel estimator having a known data input, an input coupled to receive the corresponding composite signal, an input coupled to receive the power ratio signal, and an input for receiving at least one estimate of the characteristic of the unknown data signal, estimating the at least one signal shaping characteristic of the communication channel from at least the corresponding composite signal, the at least portion of the known data signal and the at least one estimate of the unknown data signal. The channel estimator has also an output for providing at least one estimated communication channel characterizing signal; and
- An equalizer coupled to receive the corresponding signal, the known data signal, the power ratio signal, and the at least one estimated communication channel characterizing signal, configures at least one of its signal shaping characteristics to compensate for the at least one signal shaping characteristic of the communication channel, shapes the corresponding composite signal accordingly. The equalizer also has an output for providing at least subsequent estimate of the unknown data signal.

Conclusion

7. The prior art made of record and not relied upon is considered pertinent to applicant's disclosure.

US Patent Documents:

Barton et al. (US patent # 6,654,431 B1) discloses a multi-carrier personal access communication system.

Maloney et al. (US patent # 6,546,256 B1) discloses robust, efficient, location-related measurement.

Barton et al. (US patent # 6,449,246 B1) discloses a multi-carrier personal access communication system.

Jones et al. (US patent # 6,307,892 B1) discloses a multi-carrier communication system and its corresponding method for peak power control.

Humphrey et al. (US patent # 6,130,918) discloses a method and its corresponding apparatus for reducing the peak-to-average ration in a multicarrier communication system.

Bäuml et al. (US patent # 6,130,918) discloses a method and its corresponding apparatus for reducing the crest factor in digital transmission procedures.

Bottomley et al. (US patent # 5,909,465) discloses a method and its corresponding apparatus for bi-directional demodulation of digitally modulated signals.

Sakoda et al. (US patent # 5,907,583) discloses a transmitting/receiving apparatus and communicating method.

Van Nee (US patent # 5,841,813) discloses a digital communication system using complementary codes and amplitude modulation.

Other Publications:

Miolisavljevic et al., "Fixed Point Algorithm for Bit Rate Optimal Equalization in Multicarrier Systems", IEEE International Conference on Acoustics, Speech, and Signal Processing, ICASSP 1999, vol. 5, 15 – 19 March 1999, pp. 2515 – 2518.

Wang et al., "Joint Channel Estimation and Equalization in Multicarrier Modulation System Using Cyclic Prefix", IEEE International Conference on Acoustics, Speech, and Signal Processing, ICASSP 1999, vol. 5, 15 – 19 March 1999, pp. 2733 – 2736.

Contact Information

8. Any inquiry concerning this communication or earlier communications from the examiner should be directed to Dung X. Nguyen whose telephone number is (703) 305-4892. The examiner can normally be reached on Monday through Friday from 8:30 AM to 5:30 PM.

If attempts to reach the examiner by telephone are unsuccessful, the examiner's supervisor, Mr. Ghayour Mohammad H. can be reached on (703) 306-3034. The fax phone numbers for this group is (703) 872-9314.

Any inquiry of a general nature or relating to the status of this application or proceeding should be directed to the receptionist whose telephone number is (703) 305-3800.

DXN

June 15, 2004


JEAN B. CORNELIUS
PRIMARY EXAMINER

7/7/04

Notice of References Cited	Application/Control No.	Applicant(s)/Patent Under Reexamination	
	09/778,306	FARHANG-BOROUJENI ET AL.	
	Examiner Dung X Nguyen	Art Unit 2631	Page 1 of 1

U.S. PATENT DOCUMENTS

*	Document Number Country Code-Number-Kind Code	Date MM-YYYY	Name	Classification
A	US-6,654,431	11-2003	Barton et al.	375/346
B	US-6,546,256	04-2003	Maloney et al.	455/404.2
C	US-6,307,892	10-2001	Jones et al.	375/296
D	US-6,130,918	10-2000	Humphrey et al.	375/295
E	US-6,125,103	09-2000	Bauml et al.	370/203
F	US-5,909,465	06-1999	Bottomley et al.	375/227
G	US-5,907,583	05-1999	Sakoda et al.	375/260
H	US-5,841,813	11-1998	van Nee, Didier J. R	375/279
I	US-5,302,914	04-1994	Arntz et al.	330/129
J	US-6,144,860	11-2000	Komatsu, Masahiro	455/522
K	US-6,128,351	10-2000	Jones et al.	375/284
L	US-			
M	US-			

FOREIGN PATENT DOCUMENTS

*	Document Number Country Code-Number-Kind Code	Date MM-YYYY	Country	Name	Classification
N					
O					
P					
Q					
R					
S					
T					

NON-PATENT DOCUMENTS

*		Include as applicable: Author, Title Date, Publisher, Edition or Volume, Pertinent Pages)
	U	Miolisavljevic et al., "Fixed Point Algorithm for Bit Rate Optimal Equalization in Multicarrier Systems", IEEE International Conference on Acoustics, Speech, and Signal Processing, ICASSP 1999, vol. 5, 15 - 19 March 1999, pp. 2515 - 2518.
	V	Wang et al., "Joint Channel Estimation and Equalization in Multicarrier Modulation System Using Cyclic Prefix", IEEE International Conference on Acoustics, Speech, and Signal Processing, ICASSP 1999, vol. 5, 15 - 19 March 1999, pp. 2733 - 2736.
	W	
	X	

*A copy of this reference is not being furnished with this Office action. (See MPEP § 707.05(a).)
Dates in MM-YYYY format are publication dates. Classifications may be US or foreign.

FIXED POINT ALGORITHM FOR BIT RATE OPTIMAL EQUALIZATION IN MULTICARRIER SYSTEMS

Mile Milisavljević and Erik I. Verriest

Georgia Institute of Technology,

Atlanta, Georgia, USA

mm@ee.gatech.edu, erik.verriest@ee.gatech.edu

ABSTRACT

In this paper we present a fixed point algorithm for bit rate optimal time domain equalization in multicarrier systems. The algorithm outperforms standard MMSE equalizers in capacity measure. Moreover, it adaptively estimates the optimal signal delay which was an exhaustive search problem in MMSE equalizers. We briefly discuss the convergence properties and demonstrate the performance of the algorithm on a twisted pair copper wire loop with additive non-white noise.

1. INTRODUCTION

Multicarrier modulation (MCM) systems have become the technology of choice for high-speed data transmission over spectrally shaped channels. MCM transceivers divide the available frequency spectrum into a large number of parallel, independent and approximately flat subchannels, thus directly implementing the maximum likelihood (ML) detectors on the receiver side. The preferred form of multicarrier modulation is the Discrete Multitone Transform (DMT), which uses the computationally effective Fast Fourier Transform to create independent channels. Combined with the optimization of bandwidth and bit distribution across usable subchannels, this modulation scheme demonstrated the results comparable to the optimum eigendecomposition based MCM transceiver of [9, 3, 1].

The fundamental implementational difficulty of the multicarrier transmission is the intersymbol interference (ISI) which renders the subchannels mutually dependent. Intersymbol interference is usually combated by addition of the cyclic prefix whose length is equal to the channel memory, so that the output sequence seems periodic to the channel. This quasi-periodicity makes the channel description matrix circulant. In case of additive white noise, the FFT basis vectors become the eigenvectors of the channel description matrix and its eigenvalues become the DFT coefficients of its first column.

The addition of the cyclic prefix, although very efficient in decoupling the subchannels, does decrease the transmission rate, especially for the channels with long finite impulse response (FIR) and small number of DMT carriers. The equalization in MCM systems is therefore divided into two parts: time domain equalization (TEQ) and frequency domain equalization (FEQ). TEQ focuses on the task of optimally (in a certain sense) shortening of the impulse re-

sponse of the channel to the length of desired cyclic prefix, while FEQ equalizes the frequency response of the channel. After the TEQ the cyclic prefix is discarded together with the intersymbol interference contained in it.

Various approaches to the time domain equalization are possible. Due to ease of their implementation and existence of adaptive algorithms, the minimum mean square error (MMSE) algorithms are most widely used. MMSE algorithms minimize the error between the target impulse response (TIR) and the equalized channel response. The length of the target impulse response is selected to be same as the desired length of the cyclic prefix. The minimization of the mean square error therefore results in minimization of the trailing ISI in the residual energy sense. The solution of the MMSE problem for DMT transceivers exists in the closed form [9, 3]. However, this structure does not guarantee the optimality of the channel capacity, which is the approach we discuss in this paper. The channel capacity optimization algorithms have been discussed by Al-Dhahir and Cioffi [3, 1] in the form on nonlinear optimization problem. Although it has been shown that this approach has a definite performance advantage to MMSE it has also been demonstrated that it is computationally very intensive and has very uncertain convergence properties.

In this paper we analyze the problems behind the capacity optimization in more detail and reveal why most common optimization techniques fail. However, the main contribution of this paper is introduction of a fixed point technique having following benefits:

1. Guaranteed convergence to capacity optimizing values of FIR TEQ equalizer regardless of the starting point,
2. Adaptive determination of optimal signal delay, and
3. No matrix inversion and autocorrelation matrix estimation is required.

The algorithm however, does have substantial memory requirements.

2. PROBLEM ANALYSIS

The block diagram of a DMT transmission system is shown in Figure 1. A \bar{N} -point FFT is used to divide the channel spectrum into \bar{N} subchannels. For channels to be completely independent and memoryless, \bar{N} has to be infinite. In practical applications, on the other hand, \bar{N} is chosen

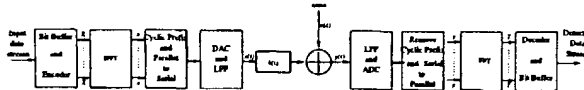


Figure 1: Block diagram of a DMT transceiver.

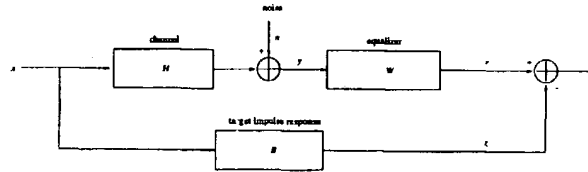


Figure 2: Block diagram of time domain equalization.

to be a power of 2. A common number used is 512. The finite number of subchannels results in the inter-block interference (IBI) which is mitigated by addition of the cyclic prefix (CP) which clears the channel memory thus making the successive block transmissions independent. Thus transformed signal is then low-pass filtered, converted to analog and sent through the channel. On the receiving side the procedure is reversed.

As we indicated before, for highly dispersive channels, the addition of the cyclic prefix whose length is same as the length of the channel response severely decreases the data rate. The solution to this problem as suggested in [9] is to linearly equalize the channel impulse response to a shorter, target impulse response (TIR). Target impulse response is chosen to be closest in the mean square error to the channel-equalizer combination as in Figure 2.

Framework we adopt is one of fractional equalization. The time domain equalizer is taken to be of length $N_f + 1$ and is denoted by vector $w = [w_0, w_1, \dots, w_{N_f}]^T$. Target impulse response is taken to be of length $N_b + 1$ and is denoted by $b = [b_0, b_1, \dots, b_{N_b}]^T$.

For any fixed b , from the orthogonality principle we have that the filter coefficients of the feed-forward equalizer w can be written as:

$$w^* R_{yy} = b^* R_{xy} \quad (1)$$

where R_{yy} and R_{xy} are the crosscorrelation matrices. This is the minimum mean square error (MMSE) solution that has been well documented in literature [9, 3, 1].

As it has been noted above, there is no guarantee that this solution will provide us with the maximum channel capacity. In order to investigate the channel capacity problem we compute the number of bits in each of \bar{N} frequency bins of DMT and sum them to obtain the number of bits transmitted in one DMT symbol:

$$b_{DMT} = \sum_{i=1}^{\bar{N}} b_i = \sum_{i=1}^{\bar{N}} \log_2 \left(1 + \frac{SNR_i}{\Gamma_i} \right) \quad (2)$$

where Γ is the signal to noise ratio gap that characterizes the distance (in dB) between SNR_i and the signal to noise ratio required to achieve the capacity and it is a function

of the probability of error, required margin and the coding gain. In order to treat all bins equally we set $\Gamma_i = \Gamma$.

The overall number of bits can be expressed as:

$$b_{DMT} = \log_2 \left(1 + \frac{SNR_{geometric}}{\Gamma} \right) \quad (3)$$

where we introduced $SNR_{geometric} = \Gamma \left[\prod_{i=1}^{\bar{N}} 1 + \frac{SNR_i}{\Gamma} \right]^{\frac{1}{\bar{N}}}$. Typically, we assume that factors "+1" and "-Γ" can be ignored and simplify the above expression to:

$$SNR_{geometric} \approx \left[\prod_{i=1}^{\bar{N}} SNR_i \right]^{\frac{1}{\bar{N}}} \quad (4)$$

Since the value of capacity is directly related to the $SNR_{geometric}$, from here on we consider only the optimization of this value. For the purpose of analysis we express the $SNR_{geometric}$ in terms of coefficients of vector b as:

$$SNR_{geometric}^n = \prod_{i=1}^{\bar{N}} SNR_i = \prod_{i=1}^{\bar{N}} \frac{b^* M_i b}{b^* N_i b} \quad (5)$$

where

$$\begin{aligned} M_i &= S_i^* \Phi_i^{bb}, \\ N_i &= S_i^* R_{xy}^* R_{yy}^{-1} \Phi_i^{ww} R_{yy}^{-1} R_{xy} + S_i^* (\Phi_i^{bb} \\ &\quad - H_i \Phi_i^{bw} R_{yy}^{-1} R_{xy} - H_i^* R_{yy}^{-1} R_{xy}^* \Phi_i^{wb} + \\ &\quad |H_i|^2 R_{yy}^* R_{xy} \Phi_i^{bb} R_{yy}^{-1} R_{xy}) \end{aligned} \quad (6)$$

and, Φ_i^{bb} , Φ_i^{ww} , and Φ_i^{bw} are the Fourier matrices such that $|B[i]|^2 = b^* \Phi_i^{bb} b$, $|W[i]|^2 = w^* \Phi_i^{ww} w$ and $W[i]^* B[i] = w^* \Phi_i^{bw} b$.

Since quantity $\frac{b^* M_i b}{b^* N_i b}$ is recognized as the Rayleigh coefficient, it follows that the vector b that maximizes the capacity for bin i is given as a solution of the generalized eigenvalue problem for the pencil $[M_i, N_i]$. Unfortunately, this conclusion cannot be generalized for the product of Rayleigh coefficients for each of the frequency bins. It is not clear whether the closed form solution for this problem exists.

Even the numerical optimization of the log-product of Rayleigh coefficients turns out to be cumbersome. First, a simple gradient optimization is computationally intensive since the gradient is given by:

$$\nabla_b SNR_{geometric} = SNR_{geometric} \left[\frac{b^* M_i}{b^* N_i b} - \frac{b^* N_i}{b^* M_i b} \right] \quad (7)$$

and, therefore, requires quadratic computational effort.

Moreover, due to the specific structure of matrices M_i , the numerator of the $SNR_{geometric}$ has numerous zeros. For example, when $N_b = 4$ (i.e. the cyclic prefix is of length 5) and for FFT length of 64, the numerator of $SNR_{geometric}$ has 101 zero eigenvalues. Moreover, matrices N_i can be poorly conditioned and may have the minimum eigenvalue close, or even equal to the small or zero eigenvalue of the numerator. Overall, this structure contributes to the very hard optimization surface with many local minima and maxima and possibly discontinuous gradients.

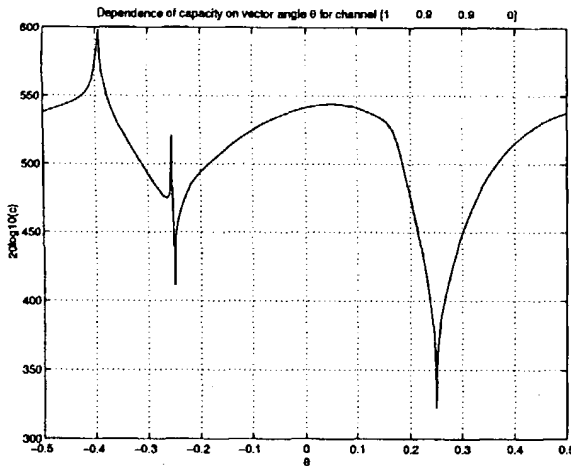


Figure 3: Dependence of capacity on the parameter $\theta = \arctan b_2/b_1$ for a simple channel.

In order to better illustrate above described behavior we performed a simple exercise that can be easily tracked analytically. We selected the order of filter b to be 2, and used a simple channel: $[1, 0.9, 0.9]$. We computed the capacity for all values of the angle θ that defines the unit norm vector \mathbf{b} as $\theta = \tan^{-1}(b_2/b_1)$. The parameter θ describes the whole space of vectors \mathbf{b} , so the optimization surface is actually a line. The dependence of the capacity on the parameter θ is shown in Figure 3.

It is obvious that for a more complex surfaces standard optimization algorithms suffer from locality problems and cannot guarantee the convergence to the optimal capacity.

3. FIXED POINT HYBRID EVOLUTIONARY ALGORITHM

3.1. Description of the Algorithm

We propose an alternative way of DMT TEQ filter design well suited for the fixed point DSP processor applications. The algorithm is a hybrid of the Simulated Annealing and Genetic Algorithms and by construction borrows the global convergence from Simulated Annealing and convergence speed from Genetic Algorithm.

We initialize the algorithm with a set (population) of N column vectors $\tau = [\mathbf{b}', \mathbf{w}', \Delta']'$ and the control parameter T . Δ here stands for the received data delay required for the best symbol alignment.

For each of the vectors we compute the capacity and rank and sort the vectors with respect to their capacity. At this point it is important to indicate that the capacity computation is not hard, nor computationally intensive since it can be performed via efficient hardware implementation of FFT.

From the sorted population of vectors we choose pairs in a top-to-bottom fashion. These pairs become parents

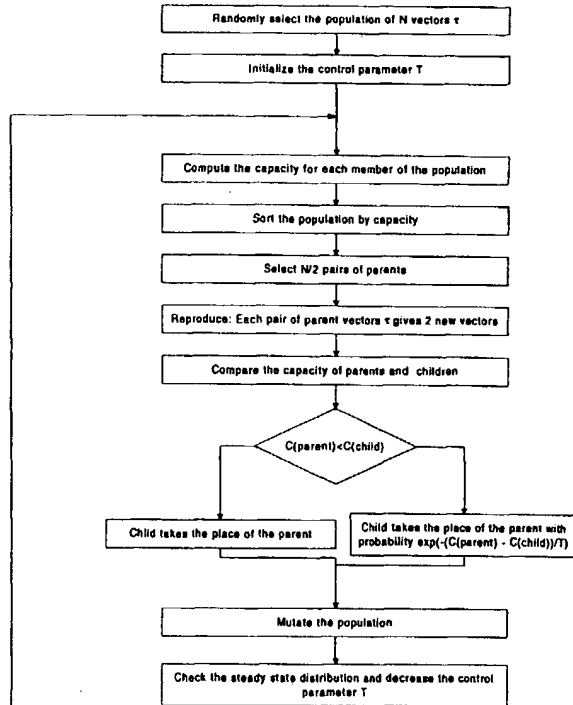


Figure 4: Flowchart of the hybrid filter design algorithm.

to new members of the population. Two new vectors are created from each set of parents by exchange of random number of bits whose position is selected at random as well. These new vectors are called children. The Boltzmann trial is held between the parents and children in following sense:

1. If the capacity of parent vector is smaller than the capacity of at least one of the children vectors, the better performing child vector takes the place of the parent.
2. If the capacity of parent vector is greater than the capacity of both child vectors, child vectors take the place of the parent with probability:

$$p = e^{-\frac{C(\tau_c) - C(\tau_p)}{T}} \quad (8)$$

We then proceed to mutate the population. This is performed by randomly selecting the pre-determined ratio of the population, and altering the random bits in the vector representation. Finally as the last step in the algorithm, we reduce the control parameter T in a logarithmic fashion.

3.2. Convergence Issues

From the description of the previous subsection it is obvious that the algorithm has strong similarities with the Simulated Annealing since it uses the probabilistic transition rule governed by the exponential of the difference between performances of the two candidates. The deviation from standard Simulated Annealing is twofold: there is $N/2$ transitions happening in every iteration (generation) and neighborhood generation is dependent on the multiple members of the population.

For the proof of convergence we use idea of [10] to concatenate all vectors τ in one large super-vector ξ . We define the performance criteria of this supervector as the sum of performances of individual vectors τ it contains. The algorithm then becomes the Simulated Annealing algorithm of [11] over the extended space of supervectors ξ and asymptotic convergence of supervectors readily follows. This, in turn, implies convergence of the population to the singular distribution at the maximum capacity point.

4. EXPERIMENTS

In order to demonstrate the effectiveness of the proposed algorithm we have implemented the algorithm for the CSA6 9kft - 26ga copper wire test line. The transmitted signal power was -40dBm which is standard for the commercial DSL services. Additive noise was modeled as ETSIB. The algorithm was initialized with initial population of 5000 vectors, and run for 100 iterations (generations). The mutation factor was constant and equal to 20% of the population vectors and 20% of the bits in the mutated vectors. The mating was performed by exchanging 40 % of randomly selected bits from both parents and each parent was paired in the Boltzmann tournament with only the child closer in the Euclidean distance to reduce the computational load.

The results of the experiment are shown in the Figure 4. The proposed algorithm clearly outperformed the MMSE as early as generation 7 and converged at generation 40 to a value close to the maximum available capacity.

5. REFERENCES

- [1] Al-Dhahir, Naofal Cioffi, John M., "Bandwidth-optimized reduced-complexity equalized multicarrier transceiver", *IEEE Trans Commun* v 45 n 8 Aug 1997 IEEE Piscataway NJ USA p 948-956.
- [2] Al-Dhahir, Naofal Cioffi, John M. "Fast computation of channel-estimate based equalizers in packet data transmission", *IEEE Trans Signal Process* v 43 11 Nov 1995 IEEE Piscataway NJ USA p 2462-2473.
- [3] Al-Dhahir, Naofal Cioffi, John M. "Optimum finite-length equalization for multicarrier transceivers", *IEEE Trans Commun* v 44 1 Jan 1996 IEEE Piscataway NJ USA p 56-64.
- [4] oois, Paul A. Lee, Inkyu Cioffi, John M., "Effect of decision delay in finite-length decision feedback equalization", *IEEE Trans Inf Theory* v 42 2 Mar 1996 IEEE Piscataway NJ USA p 618-621.
- [5] I-Dhahir, Naofal Cioffi, John M., "Symbol rate optimization for the MMSE-DFE on bandlimited dispersive channels", *Digital Signal Process Rev J* v 6 2 Apr 1996 Academic Press Inc San Diego CA USA p 73-95.
- [6] I-Dhahir, Naofal Cioffi, John M., "Efficient computation of the delay-optimized finite-length MMSE-DFE", *IEEE Trans Signal Process* v 44 5 May 1996 IEEE Piscataway NJ USA p 1288-1292.
- [7] I-Dhahir, Naofal Cioffi, John, "Optimum finite-length equalization for multicarrier transceivers", *IEEE Global Telecommun Conf* v 3 1994 IEEE Piscataway NJ USA p 1884-1888 (IEEE cat n 94CH3402-5).
- [8] I-Dhahir, Naofal Cioffi, John, "Combination of finite-length geometric equalization and bandwidth optimization for multicarrier transceivers", *Proc ICASSP IEEE Int Conf Acoust Speech Signal Process* 2 1995 IEEE Piscataway NJ USA p 1201-1204 (IEEE cat n 95CH35732).
- [9] Al-Dhahir, Naofal Cioffi, John M., "Block transmission over dispersive channels: transmit filter optimization and realization, and MMSE-DFE receiver performance", *IEEE Trans Inf Theory* v 42 1 Jan 1996 IEEE Piscataway NJ USA p 137-160, 1996.
- [10] Mahfoud, Samir, W., "Parallel Recombinative Simulated Annealing", IliGAL Report No. 93006, July 1993.
- [11] Hajek, B. "Cooling schedules for optimal annealing", *Math. of Operations Research* 13(2), p 311-329, 1988.

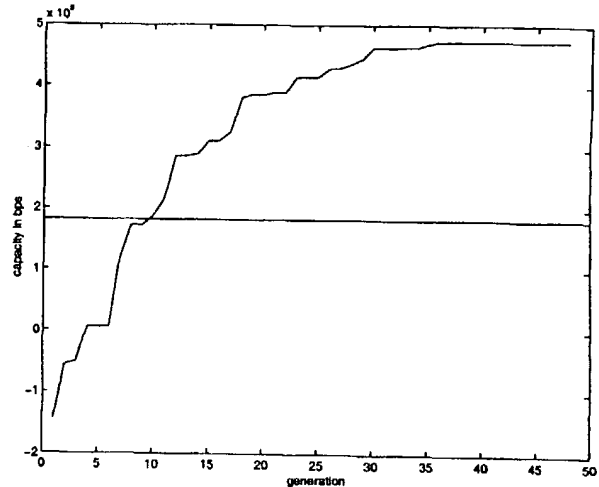


Figure 5: Comparison of the capacities achieved by MMSE equalizer design algorithm and the Simulated Annealing - Genetic Algorithm hybrid. Straight line represents the MMSE capacity which is constant with respect to iteration (generation) number. Increasing line represents the hybrid algorithm capacity which surpasses the MMSE capacity as early as 7th iteration, and rises to achieve near optimum capacity around generation 40.

JOINT CHANNEL ESTIMATION AND EQUALIZATION IN MULTICARRIER MODULATION SYSTEM USING CYCLIC PREFIX

Xiaowen Wang and K. J. Ray Liu

Electrical Engineering Department, University of Maryland
College Park, MD 20742, USA
Email: kjrliu@eng.umd.edu

ABSTRACT

Multicarrier modulation (MCM) is a promising technique for high rate data transmission. A one-tap equalizer is an essential part of the MCM system and the channel estimation is needed to get the coefficient of the equalizer. Lack of correct channel estimation may cause significant performance degradation. We propose to use the cyclic prefix to estimate the channel for the MCM system. We found that the cyclic prefix originally used solely to guarantee the optimality of modulation using discrete Fourier transform (DFT) can be viewed as a source of channel information. Based on this observation, we propose a joint channel estimation and equalization algorithm using the cyclic prefix. Our simulations show that the algorithm can adaptively track the variation of a moderately time varying channel and has about 1-2dB gain over the system using the channel estimation obtained by the conventional training schemes.

1. INTRODUCTION

Multicarrier modulation (MCM) is now considered an effective technique for high rate data communications in both wire and wireless environments. The principle of MCM is dividing the transmit data into several parallel low bit rate data streams, and using these data streams to modulate several carriers, which in frequency domain is equivalent to partition the entire channel into several parallel subchannels.

MCM provides an optimal way for channel capacity usage by adjusting the bit rate and transmit power according to the SNR of subchannels. MCM also has a relative longer symbol duration since it is a block oriented technique. The long symbol duration produces greater immunity to impulse noise and fast fading. Because of these advantages, MCM is considered a promising approach in digital subscriber line (xDSL), digital video/audio broadcasting, and wireless communications.

In MCM system, usually a one-tap equalizer is needed for each subchannel to get the estimations of transmitted data. The channel information is essential to the coefficients of the equalizers. Some techniques, such as differential PSK modulation, are used to eliminate the need for channel estimation and equalization. However, differential demodulation causes 3-4dB Signal to Noise Ratio(SNR) loss compared with coherent demodulation if channel information is known. Moreover, channel information is also very important for the bit and power allocation.

In applications such as xDSL, some training processes are performed to estimate the channel before the communication is set

up. Then, this channel estimate is used through the entire communication. If the channel changes, retraining is required to track the variation. Recently some research has been done on channel estimation and tracking in wireless communications. A minimum mean square error estimation algorithm is proposed in [5].

In this paper we propose a new channel estimation scheme that can track the change of the channel parameters without retraining. Usually a cyclic prefix or a guarding period is added between two symbols in MCM system in order to reduce the intersymbol interference (ISI). We propose to use the cyclic prefix, which is normally discarded, for channel estimation and equalization. We observed that the prefix actually provides a constantly sent training sequence if accurate transmit signal can be recovered by the conventional MCM systems. A joint channel estimation and equalization algorithm using the cyclic prefix is proposed based on this observation. Simulations were performed under the asymmetric digital subscriber line(ADSL) environment to show the effectiveness of the algorithm.

2. MCM SYSTEM USING CYCLIC PREFIX

MCM partitions a spectrally shaped channel into a number of parallel and subchannels by modulating a set of orthonormal basis functions. Most of the MCM systems choose the inverse discrete Fourier transform (IDFT) as the orthonormal basis. Fig. 1 shows a MCM system using IDFT as modulation scheme.

Input data are first buffered into blocks which are used to form the symbols transmitted in channel. Each block of data is then divided into $m/2$ bit streams in a manner determined during system initialization and mapped to some complex subsymbols to form the input of a m -point IDFT which is represented as $X_k = [X_{0,k} \ X_{1,k} \ \cdots \ X_{m-1,k}]^T$, where $X_{i,k}$ is the i th input of IDFT. The modulation is then performed by m -point IDFT and the result is $x_k = [x_{0,k} \ x_{1,k} \ \cdots \ x_{m-1,k}]^T$.

The channel is usually modeled as a FIR filter with length $v+1$. The impulse response of the channel is $h = [h_0, h_1, \dots, h_v]^T$. To reduce the ISI caused by the channel memory, a cyclic prefix $x_k^{(f)} = [x_{-v,k} \ \cdots \ x_{-1,k}]^T$, which consists of the last v samples of x_k , i.e., $x_{-i,k} = x_{m-i,k}$, $i = 1, \dots, v$, is appended in front of x_k before transmission.

At the receiver, the prefix part $y_k^{(f)} = [y_{-v,k} \ \cdots \ y_{-1,k}]^T$ is discarded, only $y_k = [y_{0,k} \ y_{1,k} \ \cdots \ y_{m-1,k}]^T$ is used for demodulation. The demodulation is performed by the DFT operation and the result is $Y_k = [Y_{0,k} \ Y_{1,k} \ \cdots \ Y_{m-1,k}]^T$.

It can be proved that the above modulation scheme is optimal due to the use of cyclic prefix in the sense that the mutual infor-

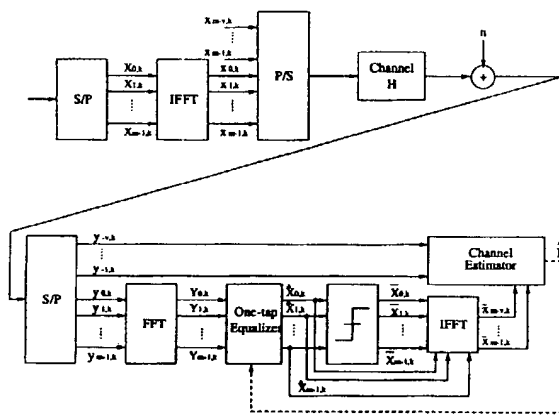


Figure 1: MCM System with Cyclic Prefix and Adaptive Channel Estimation

mation is maximized. As m goes large, the subchannels can be viewed as independent with each other, i.e.,

$$Y_{i,k} = X_{i,k} \mathcal{H}_i + N_{i,k}$$

$$\mathcal{H}_i = \sum_{l=0}^v h_l e^{-j2\pi il/m} \quad (1)$$

are samples of m point DFT of \mathbf{h} . $N_{i,k}$ are samples of m point DFT of the channel noise.

Assuming $N_{i,k}$ are independent with each other, the best estimation of $X_{i,k}$ from $Y_{i,k}$ is achieved by applying a one-tap equalizer w_i to $Y_{i,k}$, i.e.,

$$\hat{X}_{i,k} = Y_{i,k} \cdot w_i. \quad (2)$$

The optimal coefficient for the one-tap equalizer is:

$$w_i = \frac{\Gamma_i^{\frac{1}{2}} \mathcal{H}_i^*}{\Gamma_i \|\mathcal{H}_i\|^2 + \Delta_i} \quad (3)$$

where Γ_i is the transmitted power of $X_{i,k}$ and $\Delta_i = E[\|N_{i,k}\|^2]$.

Then, $\hat{X}_{i,k}$ is the hard decision result of $\hat{X}_{i,k}$, i.e., $\hat{X}_{i,k} = q(\hat{X}_{i,k})$, where $q(\cdot)$ is some kind of quantization function.

3. THE EXISTING TRAINING METHOD

The channel is modeled as the FIR filter stated before. When a training sequence x_k is sent to a channel, the output of the channel is:

$$y_k = x_k * h_k + n_k.$$

where n_k is uncorrelated random noise. Suppose \hat{h}_k is the estimation of h_k , then the estimated output $\hat{y}_k = x_k * \hat{h}_k$. The best \hat{h}_k is chosen to minimize the power of the error $\epsilon_k = y_k - \hat{y}_k$. This is the familiar quadratic form of minimizing the mean square error problem. There are many well-known methods to solve this problem, such as least squares (LS) method which is also used in our algorithm.

For MCM systems, we need to estimate the channel parameters in frequency domain. Instead of the time domain algorithm, an equivalent frequency domain deterministic least squares (DSL) channel identification algorithm can be used. In this algorithm, a training block with length m is sent periodically, and then the channel outputs are collected and averaged to reduce the influence of channel noise. The DFT of channel response is obtained by performing element by element division between the DFT of the averaged channel output and the input training sequence. Several different training blocks with guarding band can be used in order to further average out any non-linear effects. The final estimation is obtained by averaging the results of all these training blocks.

4. THE PROPOSED JOINT CHANNEL ESTIMATION AND EQUALIZATION ALGORITHM

4.1. Observation on Cyclic Prefix

The training algorithms above is designed for the time-invariant system, which means new training process must be performed if the channel varies. However, in the MCM system using cyclic prefix, we can view the cyclic prefix as a training sequence and use it to track the variation of the channel.

Let's consider the prefix part $y_k^{(f)}$ which is originally discarded. The relationship between $y_k^{(f)}$ and the transmit signal is

$$y_k^{(f)} = \mathbf{A}_k \mathbf{h} + \mathbf{n}_k^{(f)} \quad (4)$$

where

$$\mathbf{A}_k = \begin{bmatrix} x_{-v,k} & x_{m-1,k-1} & \cdots & x_{m-v,k-1} \\ \vdots & \ddots & \ddots & \vdots \\ x_{-1,k} & \cdots & x_{-v,k} & x_{m-1,k-1} \end{bmatrix}$$

and $\mathbf{n}_k^{(f)} = [n_{-v,k} \cdots n_{-1,k}]^T$.

The lower triangle part of matrix \mathbf{A}_k is composed by $x_k^{(f)}$, while the upper triangle part is composed by the last $v-1$ samples of \mathbf{x}_k . However, this last $v-1$ samples are also the elements of the prefix $\mathbf{x}_{k-1}^{(f)}$. So if all the prefix parts concatenate together as a pair of sequences $\mathbf{x}^{(f)} = \{\cdots x_{-v,k-1} \cdots x_{-1,k-1} x_{-v,k} \cdots x_{-1,k} \cdots\}$ and $\mathbf{y}^{(f)} = \{\cdots y_{-v,k-1} \cdots y_{-1,k-1} y_{-v,k} \cdots y_{-1,k} \cdots\}$, the relationship between these two satisfies

$$\mathbf{y}_k^{(f)} = \mathbf{x}_k^{(f)} * \mathbf{h}_k + \mathbf{n}_k. \quad (5)$$

If we can get accurate estimations of transmitted prefix by the conventional MCM method, i.e., we know $\mathbf{x}_k^{(f)}$, then (5) shows that $\mathbf{y}_k^{(f)}$ and $\mathbf{x}_k^{(f)}$ form a pair of training sequences that can be used to estimate the channel.

One problem here is that we can only get the estimate of this training sequence. This estimate forms a feedback loop for the channel estimation. The error incurred by the inaccurate estimation may propagate. In order to reduce the probability of error propagation the samples after hard decision, $\bar{\mathbf{x}}_k$, are used to estimate the transmit prefix. Since the prefix is a time domain signal while $\bar{\mathbf{x}}_k$ are in frequency domain, an IDFT is performed to get the time domain estimation of $\bar{\mathbf{x}}_k$.

4.2. Least Square Method to Estimate \hat{h}

Several methods have been tried to solve \hat{h} from the training sequence formed by the cyclic prefix. The following method has the best performance in simulation.

The idea of this method is trying to use LS method directly to solve (4). However, it is observed that \mathbf{A}_k is an under-determined matrix. In order to reduce the effect of random noise, we expand (4) to form the following equation:

$$\begin{bmatrix} \mathbf{y}_{k-N}^{(j)} \\ \vdots \\ \mathbf{y}_k^{(j)} \\ \vdots \\ \mathbf{y}_{k+L}^{(j)} \end{bmatrix} = \begin{bmatrix} \mathbf{A}_{k-N} \\ \vdots \\ \mathbf{A}_k \\ \vdots \\ \mathbf{A}_{k+L} \end{bmatrix} \mathbf{h} + \begin{bmatrix} \mathbf{n}_{k-N}^{(j)} \\ \vdots \\ \mathbf{n}_k^{(j)} \\ \vdots \\ \mathbf{n}_{k+L}^{(j)} \end{bmatrix}. \quad (6)$$

After arranging data to the above form, the LS solution is given by

$$\hat{\mathbf{h}} = \mathbf{A}_{N,L}^\dagger(k) \mathbf{y}_{N,L}(k)$$

where $\mathbf{A}_{N,L}(k) = [\mathbf{A}_{k-N} \cdots \mathbf{A}_k \cdots \mathbf{A}_{k+L}]^T$ and $\mathbf{y}_{N,L}(k) = [\mathbf{y}_{k-N}^{(j)} \cdots \mathbf{y}_k^{(j)} \cdots \mathbf{y}_{k+L}^{(j)}]^T$. $\mathbf{A}_{N,L}^\dagger(k)$ is the pseudo inverse of $\mathbf{A}_{N,L}(k)$ that can be obtained by performing singular value decomposition (SVD) on $\mathbf{A}_{N,L}(k)$, which is an $(N+L+1)v \times (v+1)$ matrix. Usually $N, L > 0$, so the rank of $\mathbf{A}_{N,L}(k)$ is constrained by the length of the prefix, i.e., $\text{Rank}(\mathbf{A}_{N,L}(k)) \leq v+1$.

The roles of N is some kind of similar to forgetting factor. L is used to guarantee the amount of data is enough to get an accurate estimation.

4.3. Joint Channel Estimation and Equalization Algorithm

Based on the discussion in section 4.1 and 4.2, we summarize the channel estimation and equalization algorithm as the following:

Input: received prefix part $\mathbf{y}_k^{(j)}$ and demodulated signal \mathbf{Y}_k .

Known parameters: transmitted power Γ_i and noise power Δ_i .

Selecting parameters: N and L .

Initialization: $k = 0$, an initial training is used to get the estimation of $\hat{\mathbf{h}}(0)$.

Computation: $k = 1, 2, 3, \dots$

$$\begin{aligned} \mathcal{H}_i(k-1) &= \sum_{l=0}^v \hat{h}_i(k-1) e^{-j2\pi il/m} \\ w_i(k-1) &= \frac{\Gamma_i^{\frac{1}{2}} \mathcal{H}_i(k-1)^*}{\Gamma_i \|\mathcal{H}_i(k-1)\|^2 + \Delta_i} \\ \hat{X}_{i,k} &= Y_{i,k} w_i(k-1) \\ \bar{X}_{i,k} &= q(\hat{X}_{i,k}), i = 0, 1, \dots, m-1 \\ \bar{x}_{i,k} &= \sum_{l=0}^{m-1} \bar{X}_{i,k} e^{j2\pi il/m}, i = m-v, \dots, m-1 \end{aligned}$$

If $k = nL$, where n is an integer, use $\bar{x}_{i,k}$ calculated above to form the matrix $\mathbf{A}_{N,L}(k-L)$, then,

$$\hat{\mathbf{h}}(k) = \mathbf{A}_{N,L}^\dagger(k-L) \mathbf{y}_{N,L}(k-L);$$

otherwise, $\hat{\mathbf{h}}(k) = \hat{\mathbf{h}}(k-1)$.

Here, what we present is actually a block recursive algorithm and the channel estimation is refreshed every L symbols. The symbol by symbol recursion is just the special case as $L = 1$. The reason for such a scheme is that this algorithm is a feedback scheme which combines channel estimation and equalization together. It requires more most recently data to keep on with the channel variation. Our simulation shows that both N and L should be chosen carefully to get the best performance, usually $L > 1$.

5. SIMULATION RESULTS

In our simulation, the transmit power of all the used subchannels is set to equal and fixed to 1. QAM signal is used in each subchannel. At first, some target error probability P_e is preset. Then the bit is allocated by the following error probability constraint

$$P_e \leq 4Q\left(\frac{d_i \|\mathcal{H}_i\|}{\sqrt{\Delta_i}}\right)$$

where d_i is the minimum distance between the signal points in QAM constellation of the i th subchannel.

Initially the channel transfer function is

$$H0(D) = \frac{0.1 + 0.8D^2}{1 - 1.5D + 0.54D^2}$$

The bit allocation is done according to this transfer function and will keep unchanged during the simulation. After some time, the channel transfer function will change to some $H(D)$. Two different transfer function are used for $H(D)$.

$$H1(D) = \frac{0.1 + 0.6D^2}{1 - 1.5D + 0.54D^2}$$

$$H2(D) = \frac{0.1 + 0.8D^2}{1 - 1.4D + 0.5D^2}.$$

Length of FFT is chosen as $m = 512$. White noise is used in order to simplify simulation, i.e., $\Delta_i = \Delta$.

The averaged mean square error (MSE) per subchannel is defined as

$$\text{err} = \frac{\sum_{i \in U} \text{err}_i}{|U|}$$

where $\text{err}_i = \|X_i - \hat{X}_i\|^2$ is the MSE of the i th subchannel and U is the set of all the used subchannels. $|U|$ is the number of all the used subchannels.

In our algorithm, first 2 frames of data are sent as pure training sequence to get the initial channel estimation. After that, the real data are sent and the joint channel estimation and equalization algorithm is used to track the variation of the channel. Fig. 2-4 show the results of the simulation. The solid lines in Fig. 2 and 4 show the result of the joint channel estimation and equalization algorithm. The DSL channel identification algorithm is also performed for comparison. The dashed lines show the result of using the channel estimation obtained by DSL for $H0(D)$ without re-training when channel changes, while the dash-dot lines show that of using the channel estimation obtained by DSL for $H(D)$ when channel changes. However, the training processes are not represented in the following simulation results, since the block lengths of the training sequence and data transmission are different. It should be noted that only the channel estimations obtained by DSL are used in the following simulation and extra training sequences are needed in order to get those estimations.

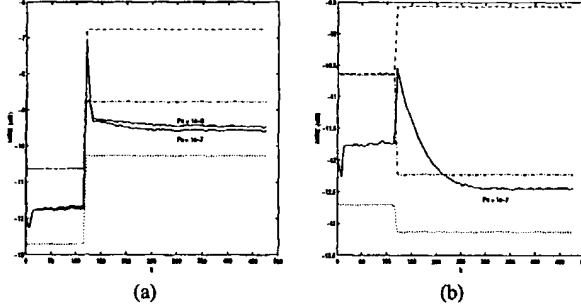


Figure 2: Average MSE per Subchannel ($\Delta = 0.01, v = 128$)

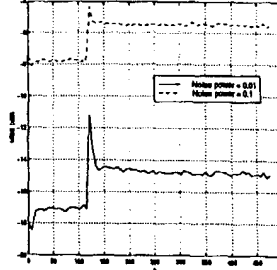


Figure 3: MSE of the 88th Subchannel ($P_e = 10^{-7}, v = 128$)

In Fig. 2, the length of the prefix is 128. N and L are 2 and 5 respectively. The average MSEs per subchannel are plotted. The channel changes from $H0(D)$ to $H1(D)$ in Fig. 2(a) while it changes to $H2(D)$ in Fig. 2(b). We can see that the algorithm converges when the channel varies. However, it converges faster in (a), in about 10 symbols, than in (b), in about 100 symbols. If we consider that the channel change is more dramatic in (b) than in (a), the result is satisfiable. Moreover, the algorithm can not only track the channel variation but also achieve about 1dB gain over the DSL method. In Fig. 2(a) the MSEs are plotted for both the target $P_e = 10^{-7}$ and $P_e = 10^{-3}$. In both cases, all 256 subchannels are used and the SNRs of each subchannel are identical. The only difference between these two cases is the minimum distance between the signal points, which means the errors of the estimation for the transmit prefix are different. The results shows that the adaptive algorithm is robust enough to such an estimation error. The MSE of $P_e = 10^{-3}$ is only a slightly larger than that of $P_e = 10^{-7}$.

In Fig. 3, the MSE of the 88th subchannel are plotted for noise power $\Delta = 0.01$ and 0.1 respectively, which means the SNR of this subchannel as $\Delta = 0.01$ is 10dB higher than that as $\Delta = 0.1$. This difference is compatible with the MSE difference in Fig. 3. As SNR goes down, the MSE is mainly caused by noise and the degradation brought by the inaccurate channel estimation becomes smaller.

Fig. 4 shows the result with much shorter length of prefix, $v = 64$. N and L are chosen as 4 and 7. The other conditions of Fig. 4 are the same as those in Fig. 2 and the result is also similar. The performance gain over the DSL reaches 2dB which is even larger compared to the case with longer prefix length. However, the algorithm converges slower, in more than 100 symbols. This is because we need to collect more symbols to get an accurate estimation, i.e., since v is small, N and L must be large to maintain the dimension of $\mathbf{A}_{N,L}(k)$ to some level. If N and L are too small, the channel estimation error becomes large enough to cause the error propagation through the equalization and the algorithm can not converge. As the prefix length goes even smaller, the error brought by the channel memory becomes too large that will also make the adaptive algorithm collapses. The smallest number we tried in our simulation that can still make the algorithm converge is 32.

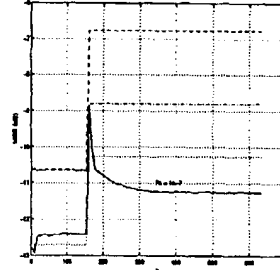


Figure 4: Average MSE per Subchannel ($\Delta = 0.01, v = 64$)

6. CONCLUSION

We have presented a joint channel estimation and equalization algorithm using the cyclic prefix in MCM system. This algorithm can adaptively track variation of a moderately time varying channel without additional training. Moreover, it also can give about 1-2dB improvement over the conventional training schemes.

7. REFERENCES

- [1] John A. C. Bingham, "Multicarrier Modulation for Data Transmission: An Idea Whose Time Has Come", *IEEE Communications Magazine*, May, 1990, pp5-14.
- [2] John M. Cioffi, *A Multicarrier Primer*.
- [3] Sanjay Kasturia, James T. Aslanis and John M. Cioffi, "Vector Coding for Partial Response Channel", *IEEE Transaction on Information Theory*, v. 36, N. 4, July 1990, pp741-762.
- [4] Jerome C. Tu, *Theory, Design and Application of Multi-Channel Modulation for Digital Communications*, Ph.D dissertation, Stanford University, June, 1991.
- [5] Ye Li, Leonard J. Cimini, Jr, and Nelson R. Sollenger, "Robust Channel estimation for OFDM Systems with Rapid Dispersive Fading Channels", *IEEE Transaction on Communications*, v. 46, N. 7, July 1998, pp902-915.